Shell-model predictions for ^{41,42}Cl(β^-)^{41,42}Ar and the A =41–43 Ar isotopes

E. K. Warburton
Brookhaven National Laboratory, Upton, New York 11973
(Received 03 April 1991)

Shell-model calculations in the model space of the $(0d, 1s)$ and $(0f, 1p)$ major shells are made for the $\frac{1}{2}^+$ and $\frac{3}{2}^+$ states of ^{41}Cl, the odd-parity states of ^{41}Ar, and the even-parity states of ^{42}Ar. Calculations for ^{42}Cl, the even-parity states of ^{41}Ar, and the odd-parity states of ^{43}Ar were performed with various degrees of truncation. The results for the ^{41}Cl ground state indicate $J^\pi = \frac{3}{2}^+$ with a binding energy of −345183 keV in excellent agreement with the experimental value of −345020 ± 150 keV. The predicted binding energies of $^{41-43}$Ar are also in good agreement with experiment. The wave functions for the $A = 41$ and 42 nuclei are used to calculate first-forbidden β^--decay rates. The $\frac{1}{2}^+$ and $\frac{3}{2}^+$ states of ^{41}Ar are considered in a truncated model space and the results are used to estimate the allowed β^--decays rates of ^{41}Cl. Spectroscopic factors and electromagnetic transition rates are calculated for ^{41}Ar and compared to experiment. ^{43}Ar is predicted to have a $\frac{5}{2}^-$ ground state.

I. INTRODUCTION

Preliminary experimental results for the β^- decay of the A =41–43 Cl isotopes were reported in 1981 (Ref. [1]). These results indicate quite complex decays which cannot easily be understood or even well established without ancillary information. Since these results may be supplemented and/or modified in the near future [2, 3] it was felt desirable to publish the present shell-model results so that they would be available to aid in the interpretation of this anticipated data. Data on the A =41–43 Ar isotopes from heavy-ion fusion-evaporation studies can also be anticipated in the near future [4] and so there is also an incentive to make available shell-model predictions pertinent to those studies.

The shell-model calculations reported herein are a continuation of an ongoing investigation [5] into the structure of neutron-rich $A \sim 40$ nuclei using shell-model interactions designed to describe nuclear levels for which the nucleons occupy the seven subshells of the (sd) and (fp) major shells. Hamiltonian diagonalization is carried out in the $(1s, 0d)^{A-16-n}(0f, 1p)^n$ model space for a single value of n. This space is designated as the nfp model space. The calculations were done with the computer code OXBASH (Ref. [6]). The nuclei under consideration here have N =23–25, i.e., the calculations are in the $3fp$ through $5fp$ model spaces with two or three proton holes in the $(1s, 0d)$ shell. The J dimension $D(J)$ of these model spaces is quite large and in some cases truncation of the $sdpf$ model space is necessary. In order to provide estimates of the relative binding energies of $1\hbar\omega$ and $2\hbar\omega$ excitations of the nfp configurations, calculations were also made in a $(d_{3/2}f_{7/2})^{A-32}$ model space using the Hsieh-Mooy-Wildenthal (HMW) interaction [7] with all possible excitations from the $d_{3/2}$ to the $f_{7/2}$ orbit. The calculations in the $d_{3/2}f_{7/2}$ model spaces revealed that the $1\hbar\omega$ and $2\hbar\omega$ excitations of the lowest-lying configurations of these Cl and Ar isotopes are overwhelmingly neutron excitations. This follows the trend found for lighter sd-shell nuclei in a study of the mass anomaly centered at $A \sim 32$. (Ref. [8]). In that study a weak-coupling model of neutron mp-mh (m-particle–m-hole) excitations was used to predict the binding energies of such $m\hbar\omega$ excitations. This weak-coupling model is used to estimate the energies of the lowest-lying states of the $1\hbar\omega$ and $2\hbar\omega$ configurations of the nuclei considered here.

II. RESULTS

A. The ^{41}Cl calculation

For ^{41}Cl the low-lying levels are expected to arise from the $4fp$ model space, i.e., three proton holes in the $(1s, 0d)$ shell and four neutrons in the $(0f, 1p)$ shell. The J dimensions $D(J)$ for this model space are $D(\frac{1}{2}) = 5884, D(\frac{3}{2}) = 10830$. Diagonalization of these is possible with the computer resources available for this study. For $J^\pi = \frac{5}{2}^+ - \frac{11}{2}^+$ diagonalization is not possible, e.g., $D(\frac{5}{2}) = 14181$. The $sdpf$ calculation for $J^\pi = \frac{1}{2}^+$ and $\frac{3}{2}^+$ was done with the Warburton-Becker-Millener-Brown (WBMB) interaction [9, 5]. The HMW, WBMB, and weak-coupling (WC) predictions for excitation energies are collected in Fig. 1. It is seen that a clear prediction of $J^\pi = \frac{3}{2}^+$ is made for the ^{41}Cl ground state. The WBMB calculation gives a binding energy of −345 183 keV as compared to the experimental value from $Q(\beta^-)$ of −345 020 ± 150 keV (Refs. [10] and [11]). Thus the good agreement of WBMB binding energy predictions for the Cl isotopes [8] is extended by one more neutron number.

The WBMB wave functions are quite complex. The $\frac{3}{2}^+_1$ state is 45% $\pi d_{3/2}^{-3}\nu f_{7/2}^4$ with no other component >10%. The $\frac{3}{2}^+_2$ state is only 12% $\pi d_{3/2}^{-3}\nu f_{7/2}^4$ while the $\frac{1}{2}^+_1$ state is 58% $\pi d_{3/2}^{-2}s_{1/2}\nu f_{7/2}^4$ and 12% $\pi d_{3/2}^{-3}\nu f_{7/2}^4$ with no other component > 6%. It is difficult to make a com-

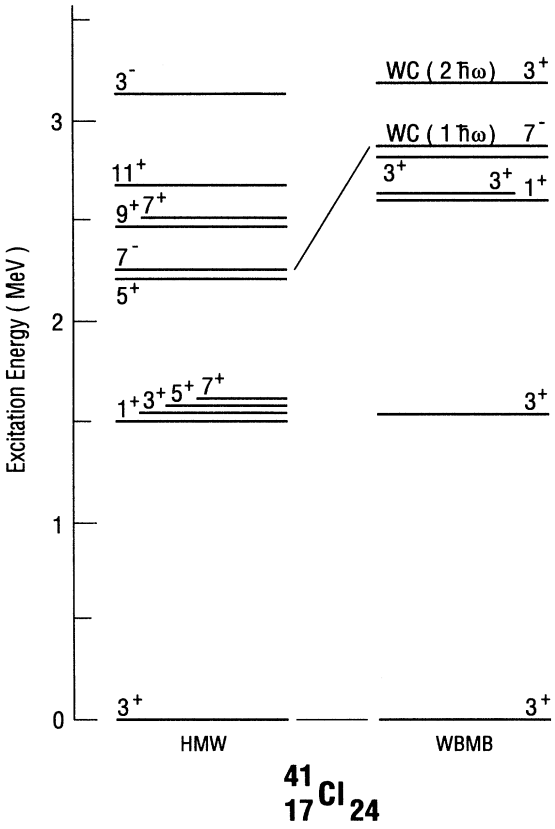

FIG. 1. Predicted energy spectrum of ^{41}Cl. Each level is labeled by $2J^\pi$. For the WBMB model, only $J^\pi = \frac{1}{2}^+$ and $\frac{3}{2}^+$ states were calculated. Weak-coupling (WC) predictions for the lowest states of the $1\hbar\omega$ $5fp$ and $2\hbar\omega$ $6fp$ configurations are also indicated.

parison of the WBMB and HMW results since the latter is confined to the $d_{3/2}f_{7/2}$ subshells but includes mp-mh excitations within that space, i.e., the HMW model space is $d_{3/2}^{5-m} f_{7/2}^{4+m}$ with $m = 0, 2, 4$.

B. The ^{41}Ar calculation

1. The $3fp$ energy spectrum

The low-lying odd- and even-parity states of ^{41}Ar are expected to be predominantly $3fp$ and $4fp$ states, respectively. Calculation of the ^{41}Ar $3fp$ spectrum in the WBMB model space is routine with a maximum $D(J)$ of 1398 for $J^\pi = \frac{7}{2}^-$. The calculated binding energy is in good agreement with experiment [8]; but the WBMB energy spectrum shows serious deficiencies [9]. It was suspected that the trouble lay in the fp part of the interaction. Accordingly, that part of the interaction was replaced with the new fp interaction FPD6 (Refs. [12] and [13]). The resulting composite $sdpf$ interaction — termed WMB — gives significantly better agreement with the ^{41}Ar energy spectrum. Results for the WMB $3fp$ energy spectrum of ^{41}Ar are listed in Table I. The predicted binding energy of the ^{41}Ar ground, −349 905 keV, is in excellent agreement with the experimental value [11] of −349 911 keV.

2. 3fp spectroscopic factors

The principal known experimental data on the spectroscopy of ^{41}Ar consists of $^{40}Ar(d,p)^{41}Ar$ spectroscopic factors [14, 15] $\hat{J}S_n^+$ ($\hat{J} \equiv 2J + 1$) and level lifetimes [16]. Thermal neutron capture provides some information on γ-ray branching ratios and the relative cross sections for primary capture [16] correlate nicely with the $\hat{J}S_n^+$ values from the (d,p) reaction. The WMB predictions for the $\hat{J}S_n^+$ are compared to the experimental $l_n = 1$ values in Fig. 2. The WMB data of Fig. 2 includes all the $\frac{1}{2}^-$ and $\frac{3}{2}^-$ levels predicted below $E_x = 4.7$ MeV and all the experimental information on $l_n = 1$ transfer. Accepting the indicated correspondence between experimental and model states, the agreement for the $\hat{J}S_n^+$ is respectable. Some discrepancies can be noted, e.g., the sharing of stripping strength for the $\frac{3}{2}_2^-$ and $\frac{3}{2}_3^-$ states and the $\frac{1}{2}_2^-$ and $\frac{1}{2}_3^-$ states (it is probable that the 3010-keV state is the $\frac{1}{2}_2^-$ state).

TABLE I. The WMB $3fp$ spectrum of ^{41}Ar. The index k orders the states of a given J^π in energy. All states are included up to the $\frac{7}{2}_6^-$ state after which only $k = 1$ and 2 states are included. The E_x entry for the ground state is the predicted binding energy.

E_x (keV)	J_k^π	k	E_x (keV)	J_k^π	k
−349 905	$\frac{7}{2}^-$	1	3 306	$\frac{1}{2}^-$	3
178	$\frac{5}{2}^-$	1	3 488	$\frac{7}{2}^-$	5
557	$\frac{3}{2}^-$	1	3 601	$\frac{3}{2}^-$	5
1 156	$\frac{3}{2}^-$	2	3 625	$\frac{9}{2}^-$	4
1 760	$\frac{11}{2}^-$	1	3 779	$\frac{5}{2}^-$	5
1 816	$\frac{9}{2}^-$	1	3 787	$\frac{7}{2}^-$	6
2 201	$\frac{1}{2}^-$	1	4 205	$\frac{13}{2}^-$	1
2 231	$\frac{5}{2}^-$	2	4 324	$\frac{13}{2}^-$	2
2 235	$\frac{7}{2}^-$	2	4 724	$\frac{15}{2}^-$	2
2 610	$\frac{7}{2}^-$	3	5 798	$\frac{17}{2}^-$	1
2 620	$\frac{9}{2}^-$	2	6 457	$\frac{19}{2}^-$	1
2 790	$\frac{3}{2}^-$	3	7 291	$\frac{17}{2}^-$	2
2 864	$\frac{5}{2}^-$	3	7 809	$\frac{19}{2}^-$	2
2 985	$\frac{1}{2}^-$	2	10 618	$\frac{21}{2}^-$	1
3 044	$\frac{3}{2}^-$	4	11 644	$\frac{21}{2}^-$	2
3 233	$\frac{11}{2}^-$	2	12 242	$\frac{23}{2}^-$	1
3 244	$\frac{5}{2}^-$	4	14 833	$\frac{23}{2}^-$	2
3 270	$\frac{9}{2}^-$	3	17 448	$\frac{25}{2}^-$	1
3 282	$\frac{15}{2}^-$	1	24 855	$\frac{25}{2}^-$	2
3 300	$\frac{7}{2}^-$	4			

3. Intruder states

Inspection of Fig. 2 reveals at least two more $\frac{1}{2}^- - \frac{3}{2}^-$ states below 4.7-MeV excitation than are predicted in the WMB $3fp$ spectrum. This raises two questions. What is the J^π and configuration of the 1635-keV level? What are the predictions for the $1\hbar\omega$ and $2\hbar\omega$ intruder states? As regards the 1635-keV level, Sen *et al.* [15] gave it a definite $\frac{3}{2}^-$ assignment. As indicated in Fig. 2, we feel some doubt should attach to this assignment. First, the (d,p) cross section leading to it is weak — as weak as to the 167-keV level to which Sen *et al.* gave an erroneous $\frac{7}{2}^-$ assignment — and, second, the most forward angle datum point in the angular distribution is in poor agreement with an $l_n = 1$ stripping pattern. As indicated in Fig. 2, both the weak-coupling and HMW predictions are that the $2\hbar\omega$ states should commence somewhat above 2 MeV. The HMW prediction is that the lowest $2\hbar\omega$ state has $J^\pi = \frac{5}{2}^-$. The weak-coupling prediction is that it has the J^π of ^{43}Ar (based on the present shell-model predictions, ^{43}Ar most probably has $J^\pi = \frac{5}{2}^-$ with $\frac{7}{2}^-$ also possible). For these reasons, it is theoretically difficult to accommodate another $\frac{3}{2}^-$ state at 1635 keV. Since the $1\hbar\omega$ states commence at 1035 keV, there are even-parity possibilities for a 1635-keV level, there are also the $\frac{9}{2}^-_1$ and $\frac{11}{2}^-_1$ possibilities (see Table I).

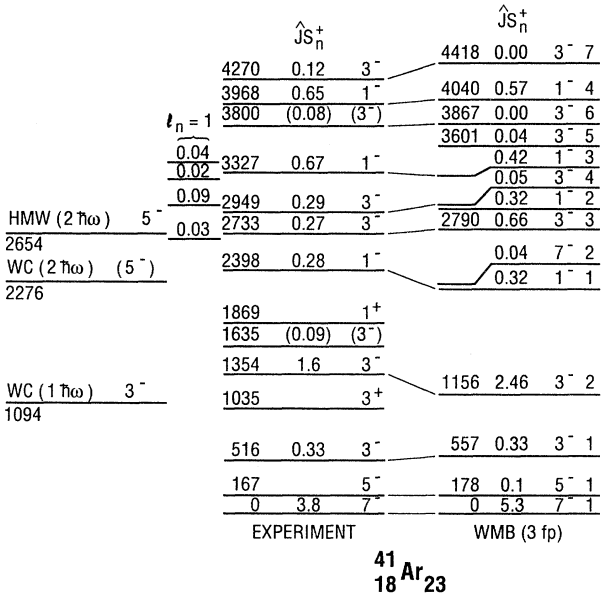

FIG. 2. Comparison of shell-model predictions to experiment for ^{41}Ar. The main emphasis is on $l_n = 1$ $\hat{J}S_n^+$ values. In addition to $\hat{J}S_n^+$, $2J^\pi$ is shown for experiment and $2J^\pi k$ for the WMB predictions, where k orders J^π states by energy. The excitation energy (in keV) is shown for most experimental states and some WMB predictions. The experimental values under the label $\hat{J}S_n^+$ are from Ref. [15]. In addition, four further $\hat{J}S_n^+$ are given to the left under the $l_n = 1$ label. These are from Ref. [14] but are scaled relative to the $\hat{J}S_n^+$ of Ref. [15] for the 1354-keV level. For experiment, all definitely known states compiled by Endt (Ref. [16]) with $E_x < 2$ MeV are shown, while for $E_x > 2$ MeV, only states observed to have $l_n = 1$ stripping patterns are included. All WMB $3fp$ $\frac{1}{2}^-$ and $\frac{3}{2}^-$ states below $E_x = 4.7$ MeV are shown. Predicted energies for the lowest state of the $1\hbar\omega$ and $2\hbar\omega$ $4fp$ and $5fp$ configurations are given on the far left and are labeled as WC (weak coupling) or HMW (see text). In addition to the $l_n = 1$ strength, Kashy *et al.* (Ref. [14]) observed a state at 3393 keV with an $l_n = 3$ $\hat{J}S_n^+$ value of ~ 0.23. The only appreciable $l_n = 3$ strength predicted below 4.7 MeV is to the ground state and to the $k = 4$ and 5 $\frac{7}{2}^-$ states at 3300 keV ($\hat{J}S_n^+ = 0.24$) and 3489 keV ($\hat{J}S_n^+ = 0.20$). An association of the 3393-keV level as the $\frac{7}{2}^-_4$ $3fp$ state seems plausible.

4. Electromagnetic transitions between the low-lying states

Predictions for the decay of four $3fp$ ^{41}Ar states are compared to experiment in Table II. The policy is to compare the most fundamental parameter possible. This is hampered by the lack of information on $E2/M1$ mixing ratios. The agreement is generally good. The worst agreements involve the $\frac{3}{2}^-_2$ state. Note that the $\hat{J}S_n^+$ value for this state is predicted to be considerably larger than the experimental value. It seems likely that the difficulty involves mixing with $5fp$ intruder states.

5. The $4fp$ $\frac{1}{2}^+$ and $\frac{3}{2}^+$ states

The $4fp$ $\frac{1}{2}^+$ and $\frac{3}{2}^+$ states have $D(J)$ values of 39927 and 73821, respectively. Thus a truncation of the *sdpf* model space is necessary in order to estimate the allowed β^--decay rates of ^{41}Cl. In OXBASH, truncation can be accomplished by selection of partitions; a partition being a specific occupancy of the subshells included in the interaction. The method of truncation used is that designated SPET by Brussaard and Glaudemans [18]. With the single-particle energy associated with the subshell j designated as $\epsilon(j)$, the zeroth-order partition energy for the kth partition was defined as

$$\mathcal{E}(k) = \left(\sum \epsilon(j)\right)_k - \left(\sum \epsilon(j)\right)_{k_0}, \qquad (1)$$

where the k_0th partition is the one with the lowest value of $\mathcal{E}(k)$ and the sums run over all active nucleons — 25 in this case. Each partition also has a J dimension, $D_k(J)$. The partitions were ordered by $\mathcal{E}(k)$ and a cutoff was imposed at the value of k, k_c, for which $\sum_{k=1}^{k_c} D_k(\frac{3}{2})$ was near the largest possible for the available disk space. This included 77 of the 337 partitions of the full $4fp$ model space and gave $\sum_{k=1}^{77} D_k(\frac{3}{2}) = 9808$. For the 77th partition the energy $\mathcal{E}(k)$ is 15.5 MeV. The calculation was performed with the WMB interaction. For clarity, the notation WMB(t) is used for truncated

TABLE II. Comparison of experimental and predicted (WMB) γ decays connecting the low-lying odd-parity ($3fp$) states of ^{41}Ar. The $B(E2)$ and $B(M1)$ are in Weisskopf units (W.u.), meanlifes are in ps, and branching ratios (B) are in percent. τ_p is the partial meanlife for the listed branch. The phase convention is that of Rose and Brink (Ref. [17]). Powers of 10 are given in square brackets and uncertainties in parentheses. The experimental information is from Ref. [16]. The $E2$ observables in the columns labeled (a) and (b) are calculated with e_p, e_n = 1.29, 0.49, and 1.35, 0.35, respectively. The $M1$ observables in column (a) use the effective g factors described in the text, while those in column (b) are calculated with the free-nucleon g factors. The results in column (a) are preferred.

Initial state		Final state		E_γ	τ	B	Quantity	Measured	Predicted values	
E_i (keV)	J_k^π	E_f(keV)	J_k^π	(keV)	(ps)	(%)		value	(a)	(b)
167	$\frac{5}{2_1}^-$	0	$\frac{7}{2_1}^-$	167	605(45)	100	$B(M1)$	11.2(8)[−3]	12.5[−3]	26.1[−3]
							$B(E2)$	a	8.67	6.84
516	$\frac{3}{2_1}^-$	0	$\frac{7}{2_1}^-$	516	475(30)	78(3)	$B(E2)$	4.36(27)	3.80	2.65
		167	$\frac{5}{2_1}^-$	349		22(3)	$B(M1)$		0.19[−3]	1.66[−3]
							$B(E2)$		4.32	2.79
							τ_p	2.2(3)[+3]	2.05[+3]	4.25[+2]
1354	$\frac{3}{2_2}^-$	0	$\frac{7}{2_1}^-$	1354	0.58(7)	3(2)	$B(E2)$	1.1(8)	1.82	1.54
		167	$\frac{5}{2_1}^-$	1187		81(2)	$B(M1)$		20.3[−3]	14.7[−3]
							$B(E2)$		2.72	2.33
							τ_p	0.72(9)	0.88	1.21
		516	$\frac{3}{2_1}^-$	838		16(2)	$B(M1)$	1.5(3)[−2]	3.76[−3]	4.65[−3]
							$B(E2)$	a	0.03	0.07
2398	$\frac{1}{2_1}^-$	167	$\frac{5}{2_1}^-$	2231	0.17(5)	5(2)	$B(E2)$	0.5(2)	1.5[−2]	2.5[−3]
		516	$\frac{3}{2_1}^-$	1882		28(4)	$B(M1)$		8.59[−3]	26.8[−3]
							$B(E2)$		5.94	5.52
							τ_p	0.6(2)	0.31	0.14
		1354	$\frac{3}{2_2}^-$	1044		67(5)	$B(M1)$		8.27[−3]	45.4[−3]
							$B(E2)$		2.72	1.75
							τ_p	0.25(8)	3.02	0.61

[a] Predicted to be negligible compared to the $M1$ contribution.

calculations. Because of the truncation, no meaningful absolute binding energies are predicted. Assuming the even-parity states commence at an excitation energy of 868 keV (giving the best average agreement with the two experimentally known even-parity states, see Table I) the relative excitation energies yield levels as follows: J^π, E_x(MeV)=$\frac{3}{2}^+$,868; $\frac{1}{2}^+$,2036; $\frac{3}{2}^+$,3266; $\frac{3}{2}^+$,3544, etc.

C. β^- decay of ^{41}Cl

1. *First-forbidden decays*

The β^- decay of ^{41}Cl was first reported by Gurach *et al.* [10] who measured $Q(\beta^-)$ to be 5670 ± 150 keV. In 1981 Huck, *et al.* [1] presented a complex decay scheme with at least fourteen decay branches and a half-life of 38.4 ± 0.8 s. However, since the decay scheme is preliminary it will not be quoted in detail.

The first-forbidden β^--decay rates for all energetically available $J^\pi \leq \frac{7}{2}^-$ states were calculated with the procedures outlined in detail previously [19]. Results were

TABLE III. Predictions for the first-forbidden decay of $^{41}Cl(\frac{3}{2}^+)$ to states of ^{41}Ar. Excitation energies are in keV. The β^- branching ratio was calculated using the experimental (expt.) excitation energy when listed and the WMB value otherwise. The total first-forbidden branching ratio was calculated to be 4.00%, i.e., 0.03% is to states not listed.

State (J_k^π)	Excitation energy expt.	WMB	logf_0t	Branching Ratio (%)
$\frac{3}{2_1}^-$	516	557	7.93	0.39
$\frac{3}{2_2}^-$	1354	1156	7.15	1.03
$\frac{3}{2_3}^-$	2733	2790	8.43	0.01
$\frac{3}{2_4}^-$	2949	3044	6.81	0.21
$\frac{3}{2_5}^-$		3601	7.31	0.02
$\frac{5}{2_1}^-$	167	178	8.02	0.42
$\frac{7}{2_1}^-$	0	0	7.43	1.86
$\frac{7}{2_2}^-$		2235	8.20	0.03
	Total			3.97

obtained with the WBMB wave function for the ^{41}Cl ground state and both WBMB and WMB wave functions for the $3fp$ ^{41}Ar states. The differences between these two sets of results were inconsequential, the WBMB $\rightarrow$ WMB results are summarized in Table III. It is seen that very little of the β^- decay of ^{41}Cl is predicted to proceed by first-forbidden branches. In fact, the prediction is that all branches observed by Huck *et al.* [1] are to even-parity states.

2. *Allowed decays*

A feature of interest in the ^{41}Cl β^- decay is that the yrast $\frac{3}{2}^+$ and $\frac{1}{2}^+$ staes at 1035 and 1869 keV have beta moments, defined by $B(GT) = 6166/f_0 t$ of < 0.002 and 0.047, respectively [1]. The calculation gives values of 0.043 and 0.041. The state-dependent effective Gamow-Teller operator described previously [5] was used in this calculation, it gives a quenching of roughly 50% over the free-nucleon results. The result for the $\frac{1}{2}^+$ state is in good agreement with experiment but the calculation completely fails to explain the small value for the $\frac{3}{2}^+$ state. The beta matrix element, $M(\mathrm{GT}) = [\hat{J}_i B(\mathrm{GT})]^{1/2}$, can be decomposed into $\nu(sd) \rightarrow \pi(sd)$ and $\nu(fp) \rightarrow \pi(fp)$ parts:

$$\begin{aligned} M(\tfrac{3}{2}^+ \rightarrow \tfrac{3}{2}^+) &= 0.548 - 0.129 = 0.419, \\ M(\tfrac{3}{2}^+ \rightarrow \tfrac{1}{2}^+) &= 0.571 - 0.154 = 0.417. \end{aligned} \tag{2}$$

The fp contribution comes from the very small proton $(sd) \rightarrow (fp)$ excitations of 5.6% and 2.6% for $\frac{1}{2}^+$ and $\frac{3}{2}^+$, respectively. That is, the $1\hbar\omega$ $\frac{1}{2}^+_1$ and $\frac{3}{2}^+_1$ states are formed predominantly by neutron excitations of the 3fp states so there is little fp proton occupancy available for the $\nu(fp) \rightarrow \pi(fp)$ β^- process. As seen in Eq. (2), the mechanism for cancellation exists so one possible explanation for the small $B(\mathrm{GT})$ value for the $\frac{3}{2}^+$ state is that the proton fp excitation is considerably larger than predicted.

D. ^{42}Cl and ^{42}Ar

1. *Energy spectra*

The $sdpf5fp$ 4^- states of ^{42}Cl have a $D(J)$ value of 44735. Thus the $sdpf$ model space was truncated in order to calculate the low-lying ^{42}Cl spectrum. The SPET method was used here also. The lowest 158 partitions of the 405 $5fp$ partitions were retained. The cutoff energy of Eq. (1) was $\mathcal{E}(1580) = 21.96$ MeV and $D(4^-)$ was reduced to 10483. The low-lying $5fp$ energy spectrum obtained from this calculation is shown in Fig. 3. The weak-coupling prediction for the 2^+ ground state of the $1\hbar\omega$ $^{35}\mathrm{Cl}(\frac{3}{2}^+) \otimes {}^{47}\mathrm{Ca}(\frac{7}{2}^-)$ excitation is 2.34 MeV; while the $2\hbar\omega$ $^{35}\mathrm{Cl}(\frac{3}{2}^+) \otimes {}^{47}\mathrm{Ca}(\frac{7}{2}^-)$ $2^- - 5^-$ centroid is predicted at 3.42 MeV. Thus it is not expected that these configurations will have a significant influence on the levels shown in Fig. 3.

The ^{42}Ar $4fp$ spectrum in the full $sdpf$ model space has a maximum $D(J)$ of 5037 for $J^\pi = 4^+$, thus diagonalization of the complete $4fp$ spectrum was possible. Results for the WMB interaction are compared to experiment in Fig. 4. The WBMB spectrum [9] does not differ in any significant manner. The binding energy predictions are $-359\,551$ and $-359\,398$ keV for WBMB and WMB, respectively, as compared to the experimental value of $-359\,340 \pm 40$ keV (Ref. [11]). As for ^{41}Cl and ^{41}Ar, the predictions are in excellent agreement with experiment. The possible $J^\pi = 0^+$ level observed experimentally at 2513 keV is identified as the ground state of the $2\hbar\omega$ $(6fp)$ configuration for several reasons. First the weak-coupling model predicts this state at 2.68 MeV and second the 0^+ state of the $2\hbar\omega$ "intruder band" is at an energy of 2121 keV in ^{40}Ar (Ref. [20]) and local systematics favors not too different a location in ^{42}Ar. The assignment of $(3^-, 4^+)$ for the 2414-keV level is from the $^{40}\mathrm{Ar}(t,p)^{42}\mathrm{Ar}$ results of Flynn *et al.* [21] who indicated a preference for the 4^+ assignment. The weak-coupling prediction for the $1\hbar\omega$ $(5fp)$ $^{37}\mathrm{Ar}(\frac{3}{2}^+) \otimes {}^{45}\mathrm{Ca}(\frac{7}{2}^-)$ $2^- - 5^-$ centroid is 4.56 MeV.

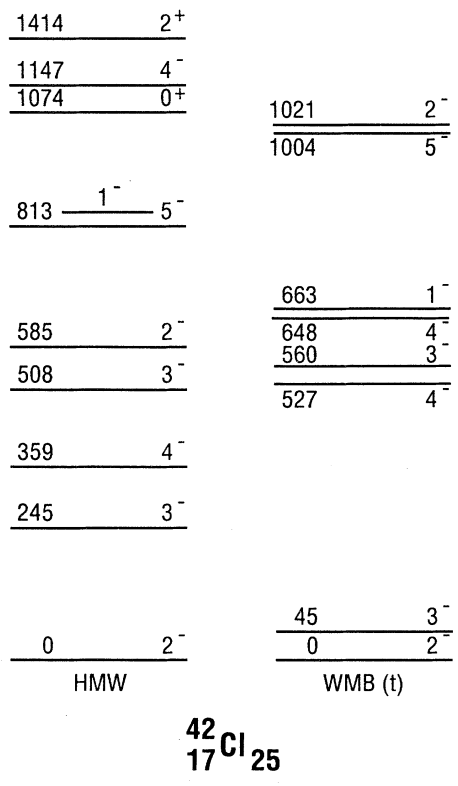

FIG. 3. Shell-model predictions for ^{42}Cl. The first eight levels are shown for the $0\hbar\omega$ $(5fp)$ WMB(t) calculation; while, for the $d_{3/2}^{5-m} f_{7/2}^{5+m}(m = 0\text{–}5)$ HMW calculation, the first ten states are shown. Excitation energies are in keV.

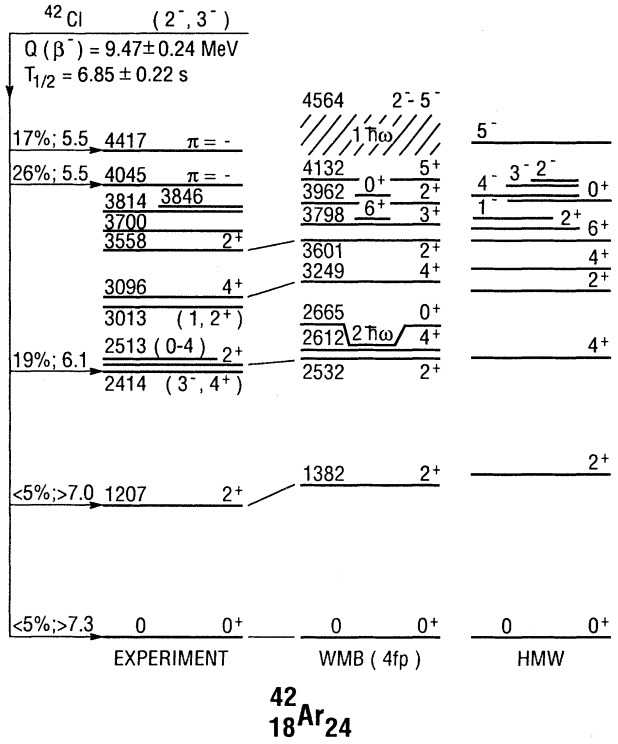

FIG. 4. Comparison of shell-model predictions to experiment for ^{42}Ar. Excitation energies are in keV. For the $0\hbar\omega$ ($4fp$) WMB calculation the first eleven levels are shown. Also included in the WMB spectrum are the $1\hbar\omega$ and $2\hbar\omega$ weak-coupling predictions. For the HMW calculation, the first eight even-parity and first five odd-parity states are shown. The experimental level scheme is from Refs. [16] and [3]. The β^- branching ratios are from Ref. [3]; for each branch the branching ratio (in percent) and the $\log f_0 t$ are listed on the left. The remaining β^--decay information is discussed in the text.

TABLE IV. Predictions for the first-forbidden decay of ^{42}Cl to states of ^{42}Ar. Excitation energies are in keV. β^- branching ratios (B) were calculated assuming both 2^- and 3^- for the ^{42}Cl ground state. The experimental (expt.) excitation energy was used when listed and the WMB value otherwise. The total first-forbidden branching ratios for $J^\pi = 2^-$ and 3^- were calculated to be 10.00% and 1.61%, respectively, i.e., 1.1% and 0.01%, respectively, are to states not listed.

State	Excitation energy		$J^\pi = 2^-$		$J^\pi = 3^-$	
(J_k^π)	expt.	WMB	$\log f_0 t$	B (%)	$\log f_0 t$	B (%)
0_1^+	0	0	7.64	2.69		
2_1^+	1207	1382	7.18	3.79	8.93	0.07
2_2^+	2485	2532	7.17	1.95	7.53	0.86
4_1^+		2612	8.24	0.16	8.77	0.05
4_2^+	3096	3249	7.79	0.28	7.55	0.34
3_1^+		3798	8.71	0.02	7.85	0.09
3_2^+		4577	8.73	0.01	7.98	0.19
	Total			8.90		1.60

2. *First-forbidden β^- decay of ^{42}Cl*

The binding energy of ^{42}Cl has been measured to be $-350\,358 \pm 220$ keV (Ref. [3]) and $-350\,848 \pm 180$ keV (Ref. [22]). The weighted average is $-350\,650 \pm 240$ keV. Together with the ^{42}Ar binding energy, this yields $Q(\beta^-) = 9472 \pm 243$ keV. The half-life of ^{42}Cl has been measured as 6.8 ± 0.3 s and 6.9 ± 0.3 s (Refs. [23] and [1]). The average of 6.85 ± 0.22 s is adopted. The first-forbidden predictions of Table IV were obtained using these experimental results and the wave functions resulting from the calculations just described. From Table IV it is seen that for either spin alternative for ^{42}Cl, the predicted branches into the yrast ^{42}Ar 0^+ and 2^+ lev-

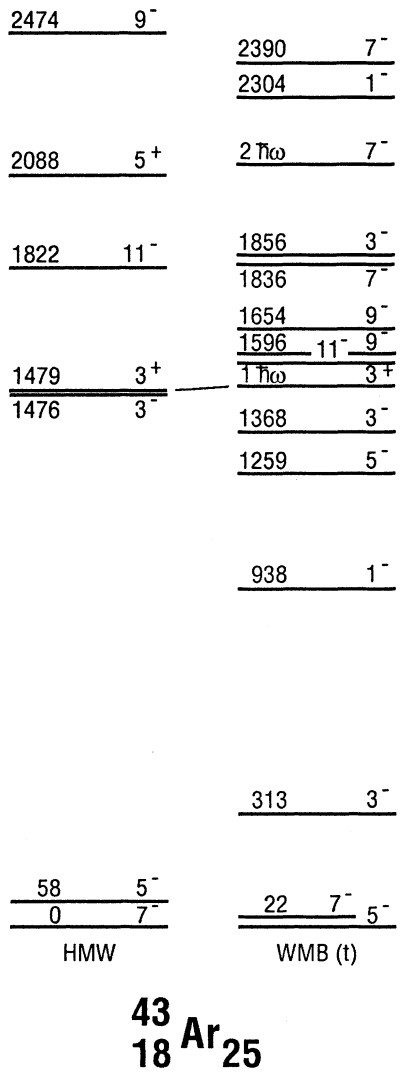

FIG. 5. Shell-model predictions for ^{43}Ar. Levels are labeled by $2J^\pi$ and by the excitation energy (in keV). Results are shown for the $0\hbar\omega$ ($5fp$) WMB(t) calculation and the $d_{3/2}^{6-m} f_{7/2}^{5+m} (m = 0\text{–}5)$ HMW calculation. For each spectrum all predicted states are shown up to the highest given. Also included in the WMB(t) spectrum are the $1\hbar\omega$ and $2\hbar\omega$ weak-coupling predictions.

TABLE V. Comparison of experimental and predicted (WMB) γ decays connecting the low-lying even-parity ($4fp$) states of ^{42}Ar. The $B(\lambda)$ are in Weisskopf units (W.u.), meanlifes are in ps, and branching ratios (B) are in percent. The phase convention is that of Rose and Brink (Ref. [17]). Powers of 10 are given in square brackets and uncertainties in parentheses.The experimental information is from Refs. [24] and [25]. The $E2$ observables in the columns labeled (a) and (b) are calculated with e_p,e_n = 1.29,0.49 and 1.35,0.35, respectively. The $M1$ observables in column (a) use the effective g factors described in Ref. [5] while those in column (b) are calculated with the free-nucleon g factors. The results of column (a) are preferred.

Initial state		Final state		E_γ	τ	B	Quantity	Measured	Predicted values	
E_i(keV)	J_k^π	E_f (keV)	J_k^π	(keV)	(ps)	(%)		Value	(a)	(b)
1208	2_1^+	0	0_1^+	1208	$3.8^{+1.0}_{-0.8}$	100	$B(E2)$	9.7(23)	6.81	5.35
2414	(4_1^+)	1208	2_1^+	1206	c	100	$B(E2)$	c	4.24	3.02
2487	2_2^+	0	0_1^+	2487	0.4 ± 0.16	17(4)	$B(E2)$	0.43(17)	0.70	0.99
		1208	2_1^+	1279		83(4)	$B(M1)$	0.031(12)	0.091	0.068
							$B(E2)$	c,d	10.34	8.58
							x($E2/M1$)	c,d	−0.250	−0.264
2513	$(0_2^+)^e$	0	0_1^+	2513	$4.0^{+3.1}_{-1.2}$	c,d	B	c,d		
		1208	2_1^+	1305		100	$B(E2)$	$6.2^{+1.2}_{-2.7}$	0.066	0.002

[c]Not measured.
[d]Assumed zero in extraction of the listed measured quantities for this level.
[e]This state is believed to be an intruder. The $4fp$ 0_2^+ state is predicted to lie at 4.03 MeV. The comparison is made to test our beliefs.

els are consistent with the experimental results recently obtained by Miehe *et al.* [3] (Fig. 4) who reevaluated the results of Huck *et al.* with the aid of some new measurements. There is one unresolved problem, namely, the large β branch into the 2414-keV level. The predictions of Table IV offer a strong argument against a 4^+ assignment for the level being feed in β^- decay. On the other hand, the model predictions for the energy spectra (Fig. 4) indicate a strong preference for the 4^+ assignment. A possibility to be considered is that there is an unresolved $3^-, 4^+$ doublet at 2414 keV. At the present time, there is no experimental preference for either the 2^- or 3^- alternatives for the ^{42}Cl ground state.

A few predictions for electromagnetic transitions in ^{42}Ar are collected in Table V. The only experimental data for the states shown is for the two 2^+ states. The agreement is only fair.

E. Energy spectrum of ^{43}Ar

The $sdpf$ $5fp$ $\frac{7}{2}^-$ states of ^{43}Ar have a $D(J)$ of 14 280. Thus the SPET method of truncation was used in the calculation of the ^{43}Ar energy spectrum. The lowest 172 of the 270 partitions of the full $5fp$ model space were retained. These gave $\sum_{k=1}^{172} D_k(\frac{7}{2}) = 9796$. For the 172th partition the energy $\mathcal{E}(k)$ is 25.7 MeV. The WMB(t) energy spectrum is shown in Fig. 5 along with the HMW predictions. The WMB(t) wave functions are quite complex with considerable participation of orbits other than $d_{3/2}$ and $f_{7/2}$. This explains the considerably higher density of levels for the WMB(t) calculation. The ^{43}Ar ground state has been assigned $J = \frac{3}{2}$ or $\frac{5}{2}$ from its decay to ^{43}K (Ref. [16]). It is pleasing that the WMB(t) calculation indicates a $\frac{5}{2}$ ground state rather than the $\frac{7}{2}$ choice which might have been *a priori* expected. In order to obtain a prediction for the binding energy of ^{43}Ar, the $\frac{5}{2}^-$ states were diagonalized in the full $5fp$ $sdpf$ basis for which $D(\frac{5}{2}^-) = 12\,138$. The result of −364 713 keV is in fair agreement with the experimental value [11] of −364 960 ± 70 keV. Note that the truncation made in the ^{43}Ar calculation is less than that in the $4fp$ ^{41}Ar and $5fp$ ^{42}Cl calculations as witnessed by the values of $\epsilon(k_c)$ of Eq. (1) which are 15.5, 22.0, and 25.7 MeV for ^{41}Ar. ^{42}Cl, and ^{43}Ar, respectively. Thus, the binding energy of ^{43}Ar resulting from the WMB(t) calculation of −364 401 keV is only 312 keV above that of the full calculation.

III. SUMMARY

For the four full $sdpf$ calculations for ^{41}Cl, and $^{41-43}$Ar, the predicted binding energies are in excellent agreement with experiment. Experimental energy spectra only are available for ^{41}Ar and ^{42}Ar. The predictions for these nuclei appear to be in good agreement with the rather sparse experimental data. For instance, if the correspondence indicated in Fig. 2 for eleven theoretical and experimental levels of ^{41}Ar is correct, the rms deviation in the excitation energy is 106 keV.

Of the nuclei considered here, ^{41}Ar is the closest to the valley of stability. Thus it is not surprising that more experimental information is available for it than the others. Previous calculations for the $3fp$ spectrum of this nucleus were performed with truncation of the $sdpf$ model space. For instance, Woods [26] used a $s_{1/2}d_{3/2}f_{7/2}p_{3/2}$ model space. Thus ^{40}Ar$(d,p)^{41}$Ar spectroscopic factors for both $p_{3/2}$ and $p_{1/2}$ orbitals could not be obtained nor could

reliable electromagnetic observables be calculated. It is found that the full *sdpf* calculation gives a satisfactory accounting of both sets of observables.

The calculation of first-forbidden β^--decay rates indicates that this mode of decay plays a minor part in the decay of ^{41,42}Cl. In fact, the prediction is that all β^- branches observed to date in these two cases are allowed decays.

It is hoped that these results [27] will stimulate further experimental effort and will aid in the interpretation of the resulting data.

ACKNOWLEDGMENTS

Research was supported by the U.S. Department of Energy under Contract Nos. DE-AC02-76CH00016.

[1] A. Huck, G. Klotz, A. Knipper, C. Miehé, C. Richard-Serre, and G. Walter, in Proceedings of the 4th Conference on Nuclei far from Stability, edited by P. G. Hansen and O. B. Nielsen, CERN Report No. 81-09, 1981 (unpublished).
[2] G. Walter, private communication, 1991.
[3] C. Miehé, Ph. Dessagne, P. Baumann, A. Huck, G. Klotz, A. Knipper, and G. Walter, Phys. Rev. C **39**, 992 (1989).
[4] D. P. Balamuth, private communication, 1991.
[5] E. K. Warburton and J. A. Becker, Phys. Rev. C **39**, 1535 (1989), and references therein.
[6] B. A. Brown, A. Etchegoyen, W. D. M. Rae, and N. S. Godwin, OXBASH, 1984 (unpublished).
[7] S. T. Hsieh, R. B. M. Mooy, and B. H. Wildenthal, Bull. Am. Phys. Soc. **30** 731 (1985); in *Nuclear Structure at High Spin Excitation and Momentum Transfer*, edited by H. Nann, AIP Conf. Proc. No. 142 (AIP, New York, 1985).
[8] E. K. Warburton, J. A. Becker, and B. A. Brown, Phys. Rev. C **41**, 1147 (1990).
[9] E. K. Warburton, J. A. Becker, D. J. Millener, and B. A. Brown, BNL Report No. 40890, 1987 (unpublished).
[10] Kh. Gurach, A. P. Kabachenko, I. V. Kuznetsov, and N. I. Tarantin, Yad. Fiz. **19**, 1167 (1974) [Sov. J. Nucl. Phys. **19**, 596 (1975)].
[11] A. H. Wapstra and G. Audi, Nucl. Phys. **A432**, 1 (1985); midstream update, P. E. Haustein, private communication, 1990.
[12] W. A. Richter, M. G. Van Der Merwe, R. E. Julies, and B. A. Brown, Nucl. Phys. **A523**, 325 (1991).
[13] The FPD6 interaction of Ref. [12] is designed to be used with a mass dependence for the two body matrix elements of $(42/A)^{0.35}$. This dependence was ignored in the present study.
[14] E. Kashy, A. M. Hoogenboom, and W. W. Buechner, Phys. Rev. **124**, 1917 (1961).
[15] S. Sen, S. E. Darden, W. A. Yoh, and E. D. Berners, Nucl. Phys. **A250**, 45 (1975).
[16] P. M. Endt, Nucl. Phys. **A521**, 1 (1990).
[17] H. J. Rose and D. M. Brink, Rev. Mod. Phys. **39**, 306 (1967).
[18] P. J. Brussaard and P.W.M. Glaudemans, *Shell-Model Applications in Nuclear Spectroscopy* (North-Holland, Amsterdam, 1977).
[19] E. K. Warburton, J. A. Becker, B. A. Brown, and D. J. Millener, Ann. Phys. (N.Y.) **187**, 471 (1988).
[20] E. Bitterwolf, A. Burkard, P. Betz, F. Glatz, F. Heidinger, Th. Kern, R. Lehmann, S. Norbet, H. Röpke, C. Schneider, and J. Siefert, Z. Phys. A **313**, 123 (1983).
[21] E. R. Flynn, O. Hansen, R. F. Casten, J. D. Garrett, and F. Ajzenberg-Selove, Nucl. Phys. **A246**, 117 (1975).
[22] D. Vieria, private communication.
[23] B. Vosicki, T. Björnstad, L. C. Carraz, J. Heinemeier, and H. L. Ravn, Nucl. Instrum. Methods **186**, 307 (1981).
[24] J. G. Pronko and R. E. McDonald, Phys. Rev. C **7**, 1061 (1973).
[25] T. R. Fisher, T. T. Bardin, J. A. Becker, and B. A. Watson, Phys. Rev. C **9**, 598 (1974).
[26] C. L. Woods, Nucl. Phys. **A451**, 413 (1986).
[27] More detailed results of the calculations described here are available on request.